Turkish Journal of Computer and Mathematics Education Vol.12 No.12 (2021), 2283-2296

Research Article

An Effective Citrus Disease Detection And Classification Using Deep Learning Based Inception Resnet V2 Model

[1]c. Senthilkumar, [2]m. Kamarasan

[1]Research Scholar, Department of Computer and Information Science, Annamalai University
[2]Assistant professor, Department of Computer and Information Science, Annamalai University

Article History: Received: 11 January 2021; Revised: 12 February 2021; Accepted: 27 March 2021; Published online: 23 May 2021

Abstract

Plant disease is a main challenge which affects the productivity and quality of the agricultural sector. The citrus plants like lemon, mandarin, orange, tangerine, grapefruit, and lime are usually grown fruits globally. The citrus production industries produce a massive quantity of waste annually where half of the citrus peel gets degraded because of various plant diseases. The recognition and classification of citrus diseases is a crucial process which improves the quality of the fruits and increase productivity. Keeping this view, this paper presented an automated citrus disease diagnosis by incorporating several processes namely preprocessing, segmentation, feature extraction, and classification. Here, Otsu based segmentation process is employed followed by ResNet with Inception v2 based feature extractor. Besides, random forest (RF) classifier is also utilized to classify the different kinds of citrus diseases. A detailed experimentation of the presented model takes place on benchmark Citrus Image Gallery dataset and the outcome pointed out the excellent disease identification and classification with the highest accuracy of 99.13%.

Keywords: Citrus disease, Deep learning, Gamma correction, Otsu method

1. Introduction

Disease caused in plants is the main problem which reduces the quality and quantity of agricultural production. Detecting and classification of plant lesion are operations done for enhancing the definition of economical growth in agriculture [1]. Citrus type of fruits is the larger form of "Rutaceae" family, which is major agriculture product globally. Some of the immediate hybrids that are typically identified in many categories like grapes, orange, limes, citrons and so on. These citrus plants affected by lesions like black spot and citrus canker. Generally, vegetables and fruits are strongly recommended for massive fiber, vitamins, and proteins that help in reducing the threat of disease attack. Among other fruits, citrus constitutes major health benefits like limonoids, flavovoids, carotenoids that denotes the stronger biological activity of citrus. Also, it contains other advantages like anti mutagenic and antioxidant properties [2]. In the year of 2010, production of citrus fruits was estimated around 122.5 million tons with the help of 8.7 million acres harvested as well as oranges were around 60% of overall cultivation. Regarding agriculture, plant diseases is been a major responsible in decreasing the production that leads for national economic loss. Citrus is mostly obtained for vitamin C around the world. Moreover, the disease for citrus directly affects the amount of production and quality. Several types of citrus plants namely oranges, grapefruit, lemons and limes are influenced with many lesions like anthracnose, scab, greening, black spot and some others are depicted in Fig. 1.

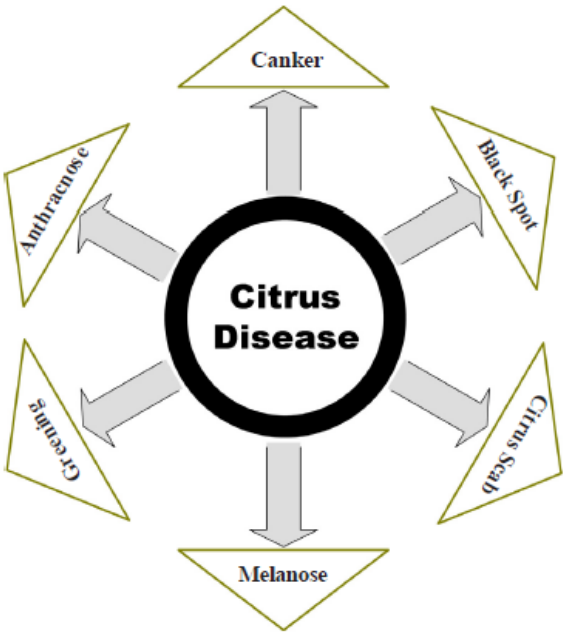

Fig. 1. Different types of citrus diseases

For detection of citrus disease, many types of methods are used like watershed, clustering, edge detection, saliency, thresholding, active contour, and some others. In every technique, detection process remains similar only with few alterations. To find a proper solution, images should be sent by 4 steps like pre-processing, segmentation, and feature extraction and classification process. Pre-processing can be used for Identifying fruits, leaves and stem affected by disease in citrus plant; Finding the disease affected area; for obtaining the shape and colour of influenced region; Discovering the solutions for citrus disease. Segmentation method performs the operation of portioning single image into different regions that has particular meaning which is utilized for feature extraction. Some of the image features are shape, colour, texture and motion relevant properties. Classification phase is applied for classifying the input data too many count of groups, simulation outcome of classification process is based on the feature selection.

Classifying models are applied to identify the images based on their extracted features. Artificial Neural Network (ANN), machine-learning technique is utilized nowadays [22-25]. MLP is the type of ANN, which changes the weight with the help of BPN training process. Many kinds of neural networks are presently utilized for texture classification [3]. RBF classification model is practical value process that is based on the provided distance. RBF is applied for Euclidean distance. It has the shape of network, where disabled units are enabled on the distance between given point and prototype point [4]. A general back propagation network is divided into 3 layers: input, hidden, and output layers. These phases are linked by the set of weight value between the nodes. BP is widely obtained to train FFNN. BP does not belong to inherent innovation analyzing; hence, it is learned while the requested outcome for training FFNNs [5]. Possible neural network (PNN) is obtained from RBF structure and it is the similar distributing processor [6]. A system is proposed for detecting the accuracy of plant diseases using ANN classification model and image processing methods. Gabor filter is utilized for feature extraction and offers effective outcome with detection rate of 91%. ANN classification is applied on various plant leaves disease and uses the texture, colour features for discovering this disease. The accuracy accomplished is around 91% [7].

k-Nearest Neighbour (KNN) is another type of geometrical classification model and applied for computing the lower distance between the actual locations to another position. The position obtained helps to estimate the distance of query image for every training image and chooses the adjacent point i.e. consist of lower distance [8]. A paper is explained with various classification models utilized for identifying plant leaves disease like ANN, kNN, PNN, PCA, SVM, fuzzy logic and genetic techniques. Classification is considered to be a model, whereas leaves are analyzed on the basis of various morphological features. The plant leaves diseases categorization is done for having an enormous application in particular region like biological research and agriculture [9]. A novel method is projected on the basis of auto white balance in images. In segmentation process, the defected area used the Euclidean Distance technique as well as applied the kNN classification unit for classifying purpose [10]. [11] discuss new model for plant leaves disease diagnosing which is based on the colour space transformation structure. Sabine and others projected a smart technique with the help of arbitrary overlapping features and affected area images are obtained with the help of K-Nearest Neighbours and Adaptive Bayes classifiers.

[12] executes the modern approach for detecting lesion in plants by using colour transformation (HSV). This is also used in segmentation process, by partitioning the infected area and uses the colour, shape and texture features for extraction of features that mostly affects the segmented area by applying K-Nearest Neighbour classifier for classifying process. [13] presented a novel method for automatic cropping leaf disease in this study. Initially, images are gathered under the state of intensity of light. For segmenting task, region of growth model is obtained on the partitioned image and PNN classification is used for dividing purpose.

In machine learning (ML), deep learning (DL) attains more attention in last few decades and accomplishes challenging solution on bigger database. Since DL is strongly used in many of ML applications. DL features are automatedly filtered from original data and train more efficient when compared with handcrafted feature. Additionally, DL resolves difficult issues with efficient and minimize the error rate. A DL scheme contains many techniques like ReLu layer, pooling layer, convolutional layer, a normalization layer, and fully connected layer [14]. In [15], establishes a Convolutional Neural Network (CNN) dependent model on previous DL namely VGG, AlexNet, GoogleNet, etc. The proposed methods are estimated on the existing database that comprises of many leaf diseases by means of healthy and non-healthy.

This paper presented an automated citrus disease diagnosis model by incorporating several processes such as preprocessing, segmentation, feature extraction, and classification. Here, Otsu based segmentation process is employed followed by ResNet with Inception v2 based feature extractor. Besides, random forest (RF) classifier is also utilized to classify the different kinds of citrus diseases. A detailed experimentation of the presented model takes place on benchmark Citrus Image Gallery dataset and the outcome pointed out the excellent classifier outcome on the applied test images over the compared models.

2. The proposed model

The working operation of the presented model for the identification of citrus disease is shown in Fig. 2. The presented model operates in several stages as explained below. As depicted, it contributes 4 major processes like pre-processing, segmentation, feature extraction, and classification. Pre-processing is done for improving the quality of the image. Then, Otsu model is used for segmenting the images. Followed by, Inception ResNet v2 model is utilized for feature extraction. Consequently, RF classification finds helpful in classifying various types of citrus diseases.

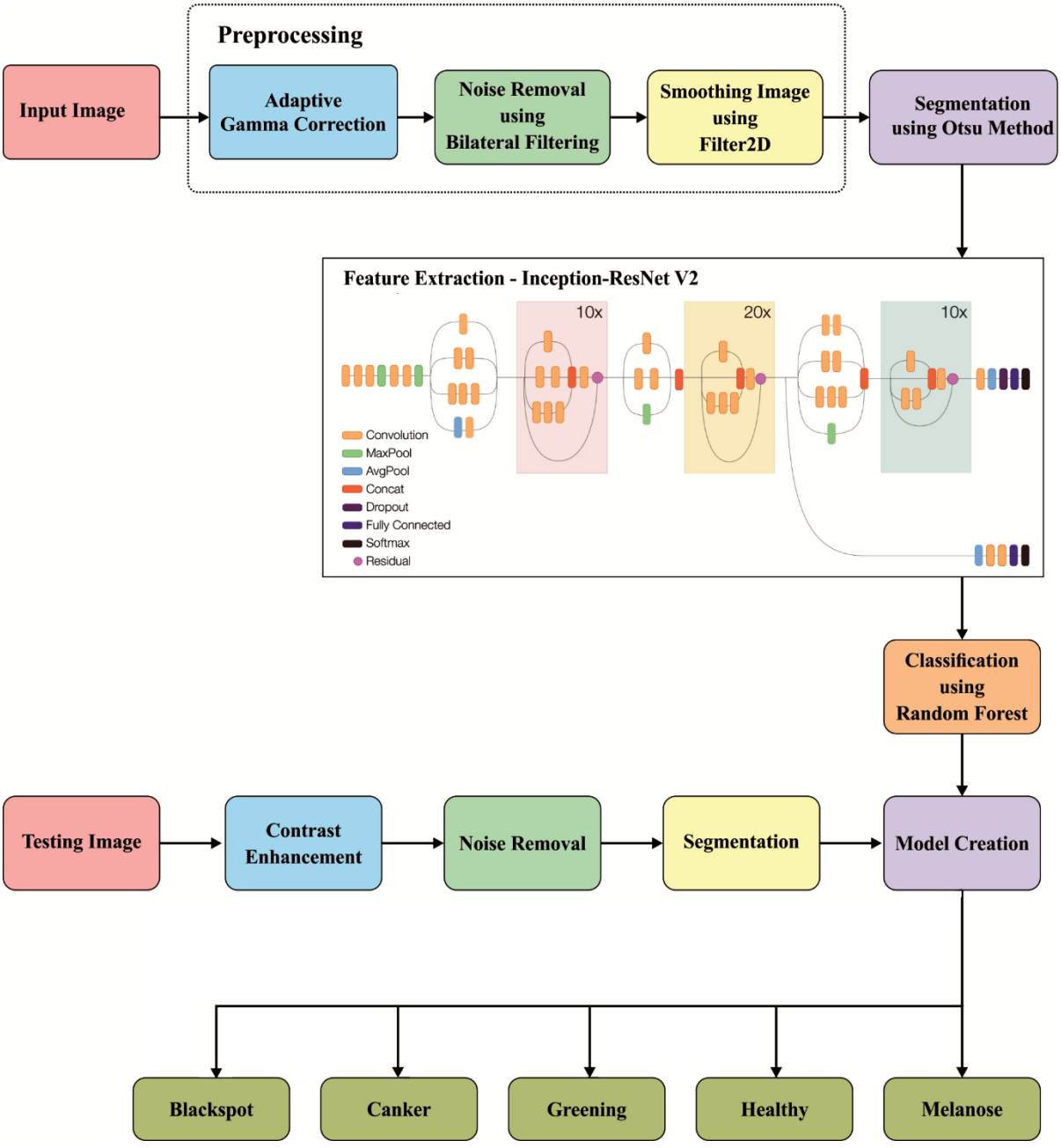

Fig. 2. Overall process of projected model

2.1. Pre processing

Pre-processing performs on 2 major levels such as Contrast Enhancement (CE) and noise removal. Initial step is CE occurs using adaptive gamma correction (AGC) technique. Secondly, noises present in the image are removed with the help of Bilateral Filtering (BF). Afterwards, smoothing of image takes place.

2.1.1. Adaptive Gamma Correction (AGC) based Contrast Enhancement (CE)

AGC technique is projected with linking gamma variable by Cumulative Distributive Function (CDF) [16]. The modified image intensity T(*i*) is estimated by

$$\mathrm{T}(i) = round\left[i_{\max}\left(\frac{i}{i_{\max}}\right)^{y(i)}\right] \quad (1)$$

$$\text{where, } y(i) = 1\text{-}\, c(i) = 1\text{-}\sum_{x=0}^{i} p\,(x) \quad (2)$$

Where $i = 0,1,..,255$, the CDF of gray levels are present in applied image, $p(x)$denotes the stable gray level histogram. *round*[·] shows rounding process. Now, 8-bit gray scale image below high pixel intensity $i_{\max} = 255$ are taken and the gamma value $y(i)$ monotonically falls from 1 to 0. The least value pixels present in minimized images would be expanded by its own.

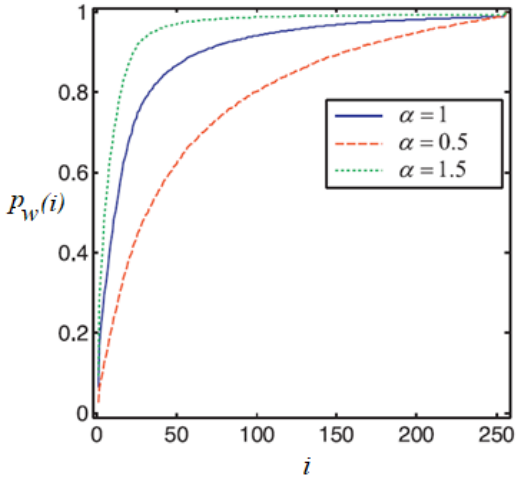

Fig. 3. AGC based CE with varying levels of α

The pixel dynamic range of end images would be transformed to covered, that CE could be reached. Therefore, a weighting distribution technique is utilized for smoothing the primary histogram as described as

$$p_w(i) = p_{\max}\left(\frac{p(i) - p_{mn}}{p_{\max} - p_{\min}}\right)^{\alpha} \quad (3)$$

where α is the modifiable parameter present in the range of 0.5 to 1.5, $p_{\max} = \max p(i)$, $p_{\min} = \min p(i)$ as given in Fig. 3. Then $p_w(i)$ are standardized yielding $p'_w(i)$. The histogram weighted using$\alpha < 1$grows relatively plane and smooth at lower intensities, so as to the adverse outcome is not stored.

2.1.2. Bilateral Filtering (BF) based Noise Reduction Process

BF is used on the gray scale images [17]. In general, few quantity of noise exists in image leads for misidentification of plant diseases. The likelihood BF is depending on specific weighting component for averaging adjacent pixels for removing noise. The general representation of BF includes, distance based domain filter part (i, i') , and a gray-value based range filter part $r((fi), (fi'))$:

$$\tilde{f}(i) = \frac{1}{N(x)}\int_{-\infty}^{\infty} f(i')d(i,i')r\big(f(i), f(i')\big)di' \quad (4)$$

where i and i' exposes the location of middle and neighbouring pixels. When the domain filter assumes a local average of adjoining pixels, range filter area enforces the value based component for eliminating filtration around the boundary. A Gaussian function is used on the basis of Euclidean pixel distance as described by

$$d(i,i') \propto \exp\left(-\frac{(i-i')^2}{2\sigma_d^2}\right) \quad (5)$$

$$r\big(f(x), f(x')\big) \propto exp\left(-\frac{\big(f(x)-f(x')\big)^2}{2\sigma_f^2}\right) \quad (6)$$

with σ_d is a width parameter of the filter kernel size and σ_f the noise standard deviation of the considered reconstructed value. The weight allocated for pixel (k,l) for denoising the pixel (i,j) is represented as

$$w(i,j,k,l) = exp\left(-\frac{(i-k)^2 + (j-l)^2}{2\sigma_d^2} - \frac{||I(i,j) - I(k,l)||^2}{2\sigma_r^2}\right)$$

where σ_d and σ_r are smoothing variables, and I(i,j) and I(k,l) are the intensity pixels are the intensity pixels (i,j) and (k,l) correspondingly.

2.1.3. Image Smoothing using Filter 2D

After the removal of noise exist in the image, smoothing of images takes place by the use of filter 2D technique. The filter2D function is applied to convolve a kernel with an image. An averaging filter can be applied on an image. A 5x5 averaging filter kernel (K) can be represented as follows.

$$K = \frac{1}{25}\begin{bmatrix} 1 & 1 & 1 & 1 & 1 \\ 1 & 1 & 1 & 1 & 1 \\ 1 & 1 & 1 & 1 & 1 \\ 1 & 1 & 1 & 1 & 1 \\ 1 & 1 & 1 & 1 & 1 \end{bmatrix} \tag{7}$$

Smoothing with the above kernel leads to the following being carried out: for every pixel, a 5x5 window is placed on this pixel, every pixel comes in the window are totalled and the sum is then divided by 25. This equates to compute the average of the pixel values exist in the window. This function takes place on every pixel present in the image for the generation of the output image.

2.2. Otsu based segmentation model

Otsu's method is deployed on various types of image processing applications for effective thresholding based image segmentation which transforms a gray scale image to a binary image. This technique considers that image embracing bi-modal histogram and evaluates optimal threshold, by splitting into inter-class or intra-class variance.:

$$\sigma_{\omega}^2(\mathrm{t}) = \omega_0(\mathrm{t})\sigma_0^2(\mathrm{t}) + \omega_{\mathrm{a}}(\mathrm{t})\sigma_{\mathrm{a}}^2(\mathrm{t}) \tag{8}$$

Aforementioned weights ω_0 and ω_{a} are probabilities of two classes independent by a threshold t and σ_0^{b} and $\sigma_{\mathrm{a}}^{\mathrm{b}}$ are the variances of these two classes. Otsu reduces the intra-class variance that is correlated to maximum inter-class variance as:

$$\sigma_{\mathrm{y}}^2(\mathrm{t}) = \sigma^2 \text{-} \sigma_{\omega}^2(\mathrm{t}) = \omega_{\mathrm{a}}(\mathrm{t})\omega_{\mathrm{b}}(\mathrm{t})[\mu_{\mathrm{a}}(\mathrm{t}) \text{-} \mu_{\mathrm{b}}(\mathrm{t})], \tag{9}$$

They are indicated by means of class possibilities ω_{a}, and class means μ_{a}.

The class probability $\omega_{\mathrm{a}}(\mathrm{t})$ will be estimated from histogram t as:

$$\omega_{\mathrm{a}}(\mathrm{t}) = \sum_0^t \mathrm{P}\,(\mathrm{i}) \tag{10}$$

where, the class mean $\mu_1(\mathrm{t})$ is:

$$\mu_{\mathrm{a}}(\mathrm{t}) = \sum_0^t \mathrm{P}\,(\mathrm{i})\mathrm{x}(\mathrm{i}) \tag{11}$$

where $\mathrm{x}(\mathrm{i})$ is the value in the middle of histogram bin. The class probabilities are determined in an iterative manner has resulted to an effective model.

2.3. Inception-ResNet v2 model

In this section, the Inception-ResNet v2 based model is applied as a feature extractor. The initial layers in the Inception-ResNet v2 model is defined for the extraction of the low level features such as dots, lines and edges. Then, the deeper layers of the network will extract the middle level features like texture, sharpness, image shadowing of particular areas of the image. Finally, the deepest layer will extract the high level features like shape to detect the presence of disease in the citrus image. For the residual version of the Inception network, simpler Inception block is employed compared to the classical Inception. Every Inception block is trailed by filter-expansion layer (1×1 convolution without activation) that is employed to increase the dimension of the filter bank prior to appending it to map the depthness of the input. It is required to give back the dimensionality minimization generated by the Inception block. A minor variation between the residual and non-residual Inception variants is that in the case of Inception-ResNet, batch-normalization is used only on top of the conventional layers, however, not on the top of summations. It is sensible to assume that a detailed usage of batch normalization is beneficial,

however, every model replica needs to train under an individual graphical processing unit (GPU). Through the avoidance of batch-normalization, the inception block count can be increased in a substantial way.

2.4. RF classifier

The extracted features from the Inception-ResNet-v2 model has been provided to the RF classifier which will classify the images into different classes. An effectual RF can be generated using the decision trees (DT) obtained from the forest. It operates on two levels. The first level builds a tree with the assistance of the instances chosen in an arbitrary way. Every tree in the forest undergo training by the use of distinct instances of identical sizes. Only partial training instances are employed to train the trees and residuals are applied for cross validation model. It is done to determine the results of the RF classifier. It is based on the concept of "robustness" of trees is balanced even at the time of declining relationship between the trees. Next, split constraints for every node in the tree are allocated as predictor variables. An essential procedure is to choose the number of variables that provides minimum association along with adequate predictive strength. So, an optimum range are attained for the subset of predictive attributes that is commonly employed for optimum test subset. At this point, a set of 2 predefined parameters are involved in the RF classifier. It makes use of GINI index for the calculation of the impurities of parameters with respect to classes. The GINI index can be determined using the following function:

$$\sum\sum_{j\neq i}\left(\frac{f(C_i,T)}{|T|}\right)\left(\frac{f(C_j,T)}{|T|}\right) \tag{12}$$

where T represents the given training dataset, C denotes the class of arbitrarily chosen case that which falls into $f(C_i,T)$, includes the likelihood of chosen values which belongs to C_i. If the determined GINI index value is enhanced, then the heterogeneity of classes gets increased. However, in case of the minimization in GINI index, then the improved, then class heterogeneity increases. But, while there is a reduction in GINI index, then heterogeneity of classes gets improved. When a child node of GINI index is smaller over parent node, then subsequent split obtained is effective. Henceforth, tree splitting could be ended at the time of GINI index achieving zero value, that represents the single class exist in each node in tree. If every tree is grown in the forest using above reasons, then classifying process takes place by the use of an effective data set.

3. Experimental Validation

3.1. Dataset Description

To examine the efficacy of the presented technique, it is validated using Citrus Image Gallery dataset. The dataset comprises a total of 609 citrus fruits images [20].

Table 1 Dataset details

Citrus Leaves	
Disease	**Number of Images**
Black Spot	171
Canker	163
Greening	204
Melanose	13
Healthy	58
Total Images	**609**

3.2. Measures

A set of measures used for analysis are false positive rate (FPR), false discovery rate (FDR), sensitivity, specificity, F-score, accuracy and kappa.

3.3. Results analysis

The efficiency of the presented model is assessed under several aspects. Table 2 displayed the images obtained from the CE process. The images in Table 2 (a-c) and (g-i) denotes the test input images. The equivalent CE images are found in the Table 2 (d-f) and (j-l) respectively. The figures clearly indicate that the contrast level of the images is clearly enhanced by the AGC method which will assist in the improvisation of classifier outcome.

Table 2 Results of Contrast Enhancement using Adaptive Gamma Correction Method

(a)	(b)	(c)
(d)	(e)	(f)
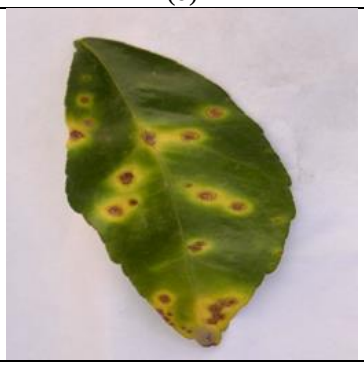		
(g)	(h)	(i)
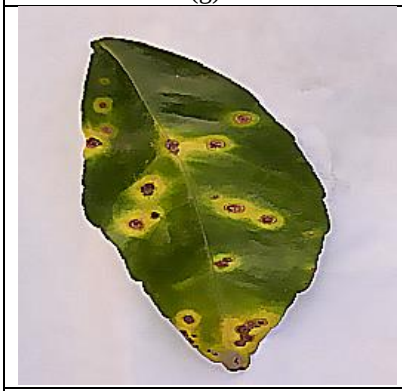		
(j)	(k)	(l)

Table 3 Segmented Images using Otsu method

(a)	(b)	(c)
		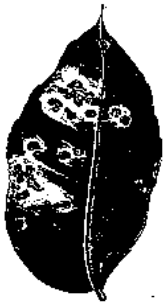
(d)	(e)	(f)
(g)	(h)	(i)
(j)	(k)	(l)

Table 3 tabulated the images attained from the Otsu based segmentation process. The images in Table 3 (a-c) and (g-i) indicates the input test images. The resultant segmented images are found in the Table 3 (d-f) and (j-l) respectively. The figures clearly point towards that the better segmentation images are found by the proposed model which will be provided as input to the proposed AGC-A model.

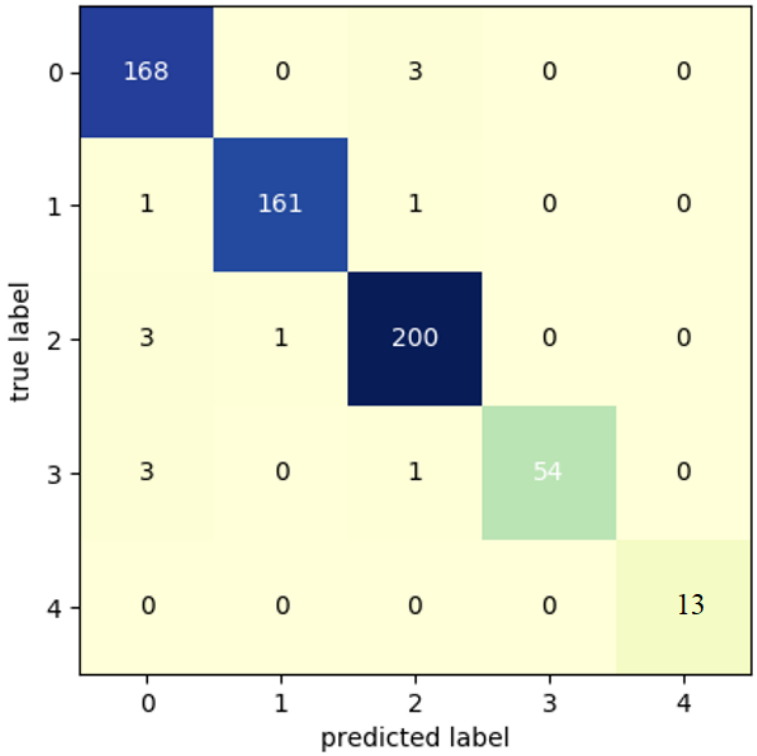

Fig. 4. Generation of Confusion Matrix at Execution Time

Fig. 4 displays the confusion matrix which is generated by the presented method. The confusion matrix in Fig. 4 is clearly represented in the form of 5*5 matrix in Table 4. The table value shows that the presented model clearly classifies a collection of 168, 161, 200, 54 and 13 images under black spot, canker, greening, healthy and Melanose type images. The values in Table 4 are manipulated in terms of TP, TN, FP and FN for determining the classifier results and is shown in Table 5.

Table 4 Confusion Matrix

Input Label	**Different Classes of Citrus Leaves**					**Total Images**
	Blackspot	**Canker**	**Greening**	**Healthy**	**Melanose**	
Blackspot	168	0	3	0	0	171
Canker	1	161	1	0	0	163
Greening	3	1	200	0	0	204
Healthy	3	0	1	54	0	58
Melanose	0	0	0	0	13	13
Total Images	175	162	205	54	13	609

Table 5 Manipulations from Confusion Matrix

Different Classes	**Blackspot**	**Canker**	**Greening**	**Healthy**	**Melanose**
TP	168	161	200	54	13
TN	428	435	396	542	583
FP	7	1	5	0	0
FN	3	2	4	4	0

Fig. 5 provided the results attained by the presented model on the identification of five different types of diseases. During the recognition of black spot disease, the presented model offered effective classification with the least FPR 1.61 and FDR of 4.00, maximum sensitivity of 98.24%, specificity of 98.39%, accuracy of 98.34%, F-score of 97.11%, G-measure of 97.12% and kappa value of 95.95% respectively. During the recognition of Canker disease, the presented model offered effective classification with the least FPR 0.22 and FDR of 0.61, maximum sensitivity of 98.77%, specificity of 99.77%, accuracy of 99.49%, F-score of 99.07%, G-measure of 99.07% and kappa value of 98.73% respectively. During the recognition of Greening disease, the presented model offered effective classification with the least FPR 1.25 and FDR of 2.43, maximum sensitivity of 98.04%, specificity of 98.75%, accuracy of 98.51%, F-score of 97.79%, G-measure of 97.79% and kappa value of 96.67% respectively. During the recognition of Healthy disease, the presented model offered effective classification with the least FPR 0 and FDR of 0, maximum sensitivity of 93.10%, specificity of 100%, accuracy of 99.33%, F-score of 96.43%, G-measure of 96.49% and kappa value of 96.06% respectively. During the recognition of Melanose disease, the presented model offered effective classification with the least FPR 0 and FDR of 0, maximum sensitivity of 100%, specificity of 100%, accuracy of 100%, F-score of 100%, G-measure of 100% and kappa value of 100% respectively. Since the values of FP attained under the Healthy and Melanose classes are zero, then the resultant FPR and FDR values also becomes to zero.

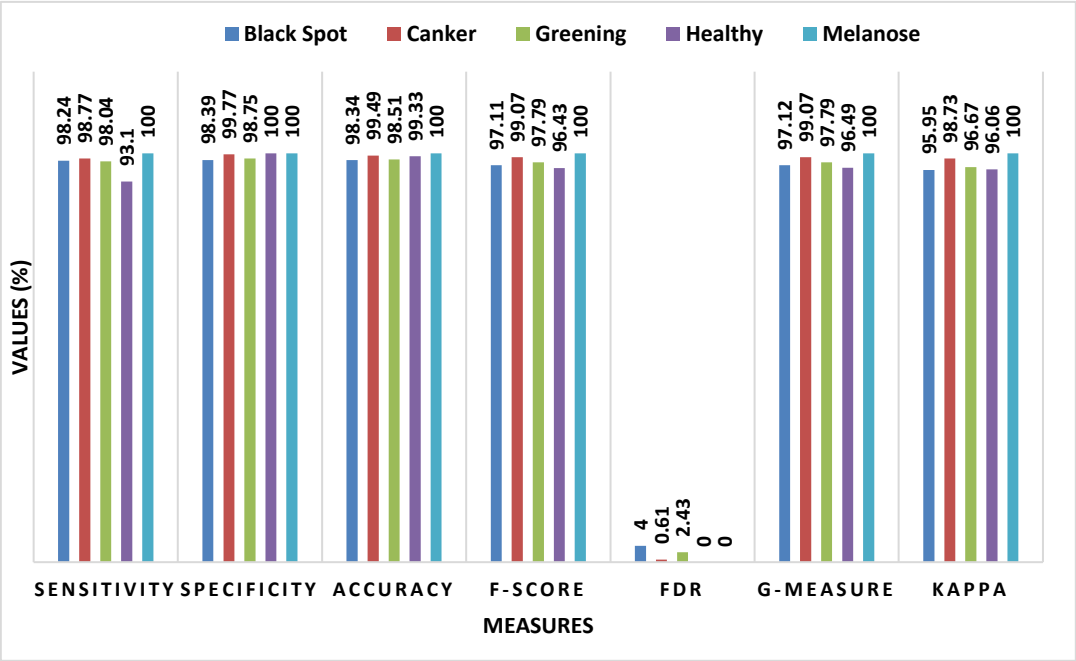

Fig. 5. Citrus disease Classification performance of proposed method

Table 6 gives the comparison of the experimental outcome achieved by distinct classifier techniques on the recognition of black spot disease with respect to FPR, FDR and accuracy. While assessing the outcome in terms of FPR, proposed model achieves an FPR of 1.61 whereas the M-SVM, W-KNN, EBT, DT and LDA offers FPR of 0.01, 0.06, 0.02, 0.02 and 0.07 respectively. Similarly, in terms of FNR, the proposed model achieves an FNR of 4.00 whereas the M-SVM, W-KNN, EBT, DT and LDA offers FPR of 1.20, 6.40, 2.5,2.5 and 6.5 respectively. With respect to accuracy, the proposed model shows most favourable black spot identification by attaining a maximum accuracy of 98.34% whereas the compared methods such as M-SVM, W-KNN, EBT, DT and LDA provide a lower accuracy of 98.70%, 93.60%, 37.40%, 97.50% and 92.30% respectively.

Table 6 Classification results of proposed with existing methods for Black Spot

Methods	**FPR**	**FDR**	**Accuracy**
Proposed	1.61	4.00	98.34
M-SVM [21]	0.01	1.20	98.70
W-KNN	0.06	6.40	93.60
EBT	0.02	2.50	97.40

DT	0.02	2.50	97.50
LDA	0.07	6.50	92.30

Table 7 gives the comparison of the experimental outcome achieved by distinct classifier techniques on the recognition of Canker disease with respect to FPR, FDR and accuracy. While assessing the outcome in terms of FPR and FDR, poor classification performance is exhibited by the EBT model by attaining a maximum FPR and FDR values of 0.03 and 3.40 respectively. In the same way, the LDA model shows better outcome over EBT model by achieving an FPR and FDR values of 0.02 and 2.60 respectively. Next to that, the W-KNN and DT models provide identical FPR and FDR values of 0.01 and 1.60 respectively. At the same time, the M-SVM model offers competitive identification outcome with the minimum FPR and FDR values of 0.009 and 0.80 respectively. But, the proposed AGC-A model provided optimal canker classification with the least FPR and FDR value of 0.22 and 0.61 respectively. With respect to accuracy, ineffective outcome is offered by EBT method with the minimum accuracy of 96.50 whereas the LDA method offers slightly higher accuracy value of 97.40. Further, the W-KNN and DT show identical results with the accuracy values of 98.30 respectively. Moreover, the presented method shows supreme Canker disease identification with the highest accuracy value of 99.49.

Table 7 Classification results of proposed with existing methods for Canker

Methods	**FPR**	**FDR**	**Accuracy**
Proposed	0.22	0.61	99.49
M-SVM	0.009	0.80	99.10
W-KNN	0.01	1.60	98.30
EBT	0.03	3.40	96.50
DT	0.01	1.60	98.30
LDA	0.02	2.60	97.40

Table 8 gives the comparison of the experimental outcome achieved by distinct classifier techniques on the recognition of Greening disease with respect to FPR, FDR and accuracy. While assessing the outcome in terms of FPR and FDR, poorer quality of identification performance is exhibited by the W-KNN model with the maximum FPR and FDR values of 0.06 and 6.20 respectively. Concurrently, the EBT and LDA models offers moderate as well as equal detection performance with the same FPR and FDR values of 0.05 and 5.10 respectively. Next to that, the DT model shows better outcome to some extent with the FPR and FDR values of 0.04 and 4.00 respectively. On continuing with, the M-SVM model offers competitive identification outcome with the minimum FPR and FDR values of 0.03 and 2.80 respectively. On the other hand, the projected AGC-A model provided most favourable Greening classification with the least FPR and FDR value of 1.25 and 2.43.

Table 8 Classification results of proposed with existing methods for Greening

Methods	**FPR**	**FDR**	**Accuracy**
Proposed	1.25	2.43	98.75
M-SVM	0.03	2.80	96.80
W-KNN	0.06	6.20	93.80
EBT	0.05	5.10	94.80
DT	0.04	4.00	95.80
LDA	0.05	5.10	94.80

With respect to accuracy, ineffective outcome is offered by W-KNN method with the minimum accuracy of 93.80% whereas the EBT and LDA method provided slightly higher accuracy value of 94.80%. Further, the DT results with the accuracy values of 95.80% respectively. Moreover, the M-SVM achieves somewhat higher accuracy value of 96.80%, the presented method shows supreme Greening disease identification with the highest accuracy value of 98.75%.

Fig. 6 gives the comparison of the experimental outcome achieved by distinct classifier techniques on the recognition of Melanose disease with respect to FPR, FDR and accuracy. While assessing the outcome in terms of FPR and FDR, LDA model exhibits worse performance by achieving a maximum FPR and FDR values of 0.08 and 7.7 respectively. At the same time, the W-KNN model shows better outcome to some extent by attaining an FPR and FDR values of 0.05 and 5.4 respectively. Next to that, the EBT and DT models shows moderate results by offering an identical FPR and FDR values of 1.25 and 2.43 respectively. On continuing with, the M-SVM model offers competitive identification outcome with the minimum FPR and FDR values of 0.03 and 2.8 respectively. On the other hand, the proposed AGC-A model provided most favourable Melanose classification with the least FPR and FDR value of 0. With respect to accuracy, ineffective outcome is offered by LDA method with the minimum accuracy of 91.30% whereas the W-KNN method provided slightly higher accuracy value of 94.20%. Further, the EBT and DT show identical results with the accuracy values of 95.70% respectively. Though the M-SVM model achieves a higher accuracy value of 97.10, it fails to outperform the proposed model which attains a maximum accuracy of 100% on Melanose disease identification.

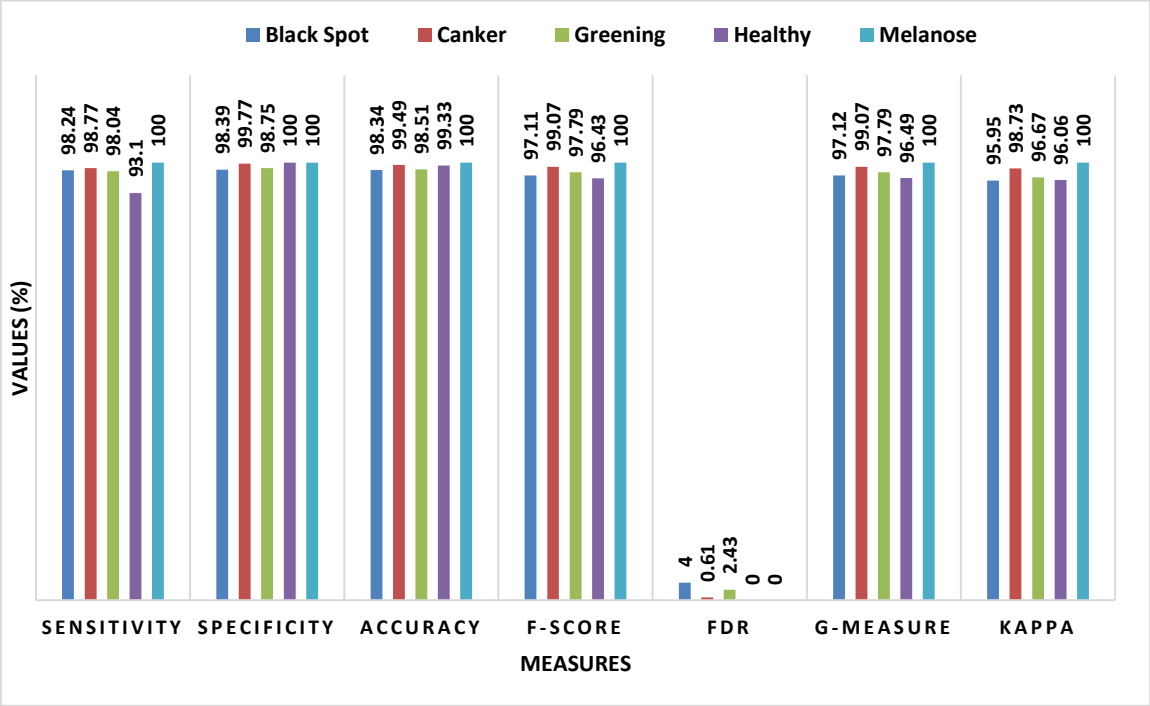

Fig. 6. Comparative analysis of different Citrus disease identification models

Fig. 7 provides a comparative analysis of proposed and existing models interms of accuracy. While assessing the outcome in terms of FPR and FDR, ineffective classifier results are offered by the LDA and W-KNN models identification performance is exhibited by the LDA and W-KNN model with the maximum over the compared ones.

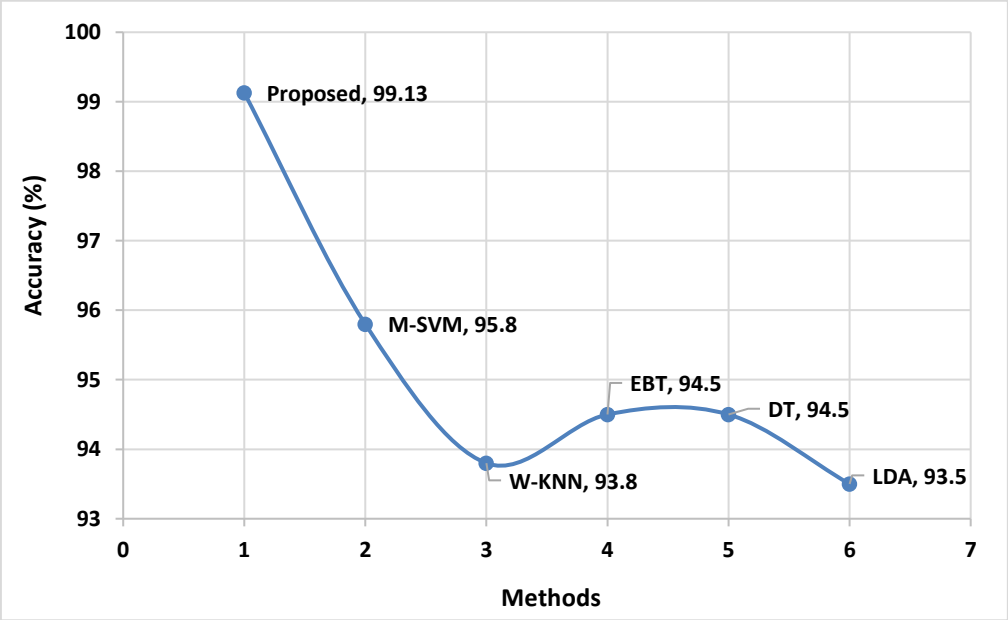

Fig. 7. Average Accuracy analysis of diverse models

On measuring the performance interms of accuracy, LDA method offers an ineffective outcome with the minimum average accuracy of 93.50% whereas the W-KNN method shows better results over LDA and provides a slightly higher average accuracy of 93.80%. At the same time, the EBT and DT models exhibits better performance over the W-KNN and LDA models by achieving a higher average accuracy 94.50% respectively. In line with, the M-SVM tries to manage well and achieves a high average accuracy value of 95.80%. However, the presented method shows supreme disease identification with the highest average accuracy value of 99.13%.

4. Conclusion

This paper has presented an automated citrus disease detection and classification model. The presented model operates in several stages as explained below. The proposed method contributes a set of 4 major processes like pre-processing, segmentation, feature extraction, and classification. Pre-processing is done for improving the quality of the image. Therefore, Otsu model is used for segmenting the images. Followed by, Inception ResNet v2 model is utilized for feature extraction. Consequently, RF classification finds helpful in classifying various types of citrus diseases. To examine the efficacy of the presented technique, it is tested against Citrus Image Gallery dataset. The simulation results pointed out that the presented model is found to be effective in the detection and classification of citrus diseases. In future, the performance of the proposed model can be further enhanced by the use of hyper parameter tuning models.

References

[1] Gutte, Vitthal S., Gitte, Maharudra A., 2016. A survey on recognition of plant disease with help of algorithm. Int. J. Eng. Sci. 7100.

[2] Sebastian, Kate (Ed.), 2014. Atlas of African Agriculture Research and Development: Revealing Agriculture's Place in Africa. Intl Food Policy Res Inst.

[3] Zhihua, Diao, Huan, Wang, Yinmao, Song, Yunpeng, Wang, 2013b. Image segmentation method for cotton mite disease based on color features and area thresholding. J. Theor. Appl. Inform. Technol. 48 (1).

[4] Kai, Song, Zhikun, Liu, Hang, Su, Chunhong, Guo, 2011. A research of maize disease image recognition of Corn Based on BP Networks. In: Third International Conference on Measuring Technology and Mechatronics Automation, Shenyang, China, pp. 246–249.

[5] Wang, Haiguang, Li, Guanlin, Ma, Zhanhong, Li, Xiaolong, 2012. Image recognition of plant diseases based on principal component analysis and neural networks. In: 8th International Conference on Natural Computation, Chongqing, China, pp. 246–251.

[6] Solankia, U., Jaliya, U.K., Thakore, D.G., 2015. A survey on detection of disease and fruit grading. Dept. Comput. Sci., ijiere 2 (2).

[7] Sannakki, S.S., Rajpurohit, V.S., 2015. Classification of pomegranate diseases based on back propagation neural network. Int. J. Adv. Found. Res. Comput. (IJAFRC)(2).

[8] Wang, Haiguang, Li, Guanlin, Ma, Zhanhong, Li, Xiaolong, 2012. Image recognition of plant diseases based on back propagation networks. In: 5th International Congress on Image and Signal Processing, Chongqing, China, pp. 894–900.

[9] Fern, Marco Antonio Aceves, Arregu, Juan Manuel Ramos, 2016. KNN-based image segmentation for grapevine potassium deficiency diagnosis. In: 2016 International Conference on Electronics, Communications and Computers (CONIELECOMP). IEEE, pp. 48–53.

[10] Prasad, Shitala, Peddoju, Sateesh K., Ghosh, Debashis, 2016a. Multi-resolution mobile vision system for plant leaf disease diagnosis. SIViP 10 (2), 379–388.

[11] Bauer, Sabine D., Kor, Filip, Frstner, Wolfgang, 2011a. The potential of automatic methods of classification to identify leaf diseases from multispectral images. Precision Agric. 12 (3), 361–377.

[12] Zhang, S.W., Shang, Y.J., Wang, L., 2015. Plant disease recognition based on plant leaf image. JAPS, J. Animal Plant Sci. 25 (Suppl. 1), 42–45.

[13] Ram Dubey, Shiv, Singh Jalal, Anand, 2012. Detection and classification of apple fruit diseases using complete local binary patterns computer and communication technology. In: 2012 Third International Conference (IEEE), 23–25 Nov, pp. 346–351.

[14] Kamilaris, Andreas, Prenafeta-Bold, Francesc X., 2018. Deep learning in agriculture: a survey. Comput. Electron. Agric. 147, 70–90.

[15] Ferentinos, Konstantinos P., 2018. Deep learning models for plant disease detection and diagnosis. Comput. Electron. Agric. 145, 311–318.

[16] Cao, G., Huang, L., Tian, H., Huang, X., Wang, Y. and Zhi, R., 2018. Contrast enhancement of brightness-distorted images by improved adaptive gamma correction. *Computers & Electrical Engineering*, *66*, pp.569-582.

[17] Tomasi, C. and Manduchi, R., 1998, January. Bilateral filtering for gray and color images. In Sixth international conference on computer vision (IEEE Cat. No. 98CH36271) (pp. 839-846). IEEE.

[18] Szegedy, C., Vanhoucke, V., Ioffe, S., Shlens, J. and Wojna, Z., 2016. Rethinking the inception architecture for computer vision. In *Proceedings of the IEEE conference on computer vision and pattern recognition* (pp. 2818-2826).

[19] Millard, K. and Richardson, M., 2015. On the importance of training data sample selection in random forest image classification: A case study in peatland ecosystem mapping. *Remote sensing*, *7*(7), pp.8489-8515.

[20] Citrus Diseases Image Gallery, December 20, 2017. [Online] Avaible http://idtools.org/ id/citrus/diseases/gallery.php.

[21] Sharif, M., Khan, M.A., Iqbal, Z., Azam, M.F., Lali, M.I.U. and Javed, M.Y., 2018. Detection and classification of citrus diseases in agriculture based on optimized weighted segmentation and feature selection. *Computers and electronics in agriculture*, *150*, pp.220-234.

[22] Alqaralleh, B. A., Vaiyapuri, T., Parvathy, V. S., Gupta, D., Khanna, A., & Shankar, K. (2021). Blockchain-assisted secure image transmission and diagnosis model on Internet of Medical Things Environment. Personal and Ubiquitous Computing, 1-11.

[23] Shankar, K., & Perumal, E. (2020). A novel hand-crafted with deep learning features based fusion model for COVID-19 diagnosis and classification using chest X-ray images. Complex & Intelligent Systems, 1-17.

[24] Bharathi, R., Abirami, T., Dhanasekaran, S., Gupta, D., Khanna, A., Elhoseny, M., & Shankar, K. (2020). Energy efficient clustering with disease diagnosis model for IoT based sustainable healthcare systems. Sustainable Computing: Informatics and Systems, 28, 100453.

[25] Anupama, C.S.S., Sivaram, M., Lydia, E.L. et al. Synergic deep learning model–based automated detection and classification of brain intracranial hemorrhage images in wearable networks. Pers Ubiquit Comput (2020). https://doi.org/10.1007/s00779-020-01492-2